International Journal of Innovative
Computing, Information and Control
Volume **12**, Number **4**, August **2016**

ICIC International ©2016 ISSN 1349-4198
pp. 1241–1255

SPECIFIED ORDER – H_∞ LOOP SHAPING CONTROL FOR HARD DISK DRIVE SERVO USING PSO

Poom Konghuayrob and Somyot Kaitwanidvilai

Department of Electrical Engineering
Faculty of Engineering
King Mongkut's Institute of Technology Ladkrabang
Chalongkrung Rd., Ladkrabang, Bangkok 10520, Thailand
poom.konghuayrob@gmail.com; drsomyotk@gmail.ac.th

Received November 2015; revised April 2016

Abstract. *The demand of data storage density has been increasing continuously, but the data access time and track pitch need to be decreased. The high precision servo control system is required to achieve the predicted goal that will be crossing 10 TB/in^2 areal density before 2020. Due to the fact that the precision of read/write head is sensitive to disturbance and noise, it is the challenging problem for the practical control. To overcome this problem, this paper proposes a new servo controller designed, specified order – H_∞ loop shaping (SOHLS) which adapts the particle swarm optimization (PSO) for searching the optimal controller parameters. The proposed technique can solve the problem of high order that was caused from the conventional H_∞ loop shaping (HLS), in addition, it can guarantee the robustness of the servo system. Based on simulation results, the performances of the proposed SOHLS approach are investigated in comparison with that of the conventional H_∞ robust loop shaping, fixed-structure H_∞ control based on non-smooth algorithm including reduced order controller by Hangkel norm model reduction technique. The proper repeatable runout (RRO) and non-repeatable runout (NRRO) were applied to the system to verify the robustness of all designed controllers. The results demonstrate the advantages of the proposed SOHLS which gains better performance and more robustness than the other conventional controllers.*

Keywords: Specified order – H_∞ robust control, Particle swarm optimization, VCM actuator, Hard disk drive, Resonance frequency

1. **Introduction.** Nowadays hard disk drive (HDD) is one of the most important technologies for developing and researching high precise industry technologies. Among the essential technologies of hard disk drive with increasing high areal density (AD), high performance control systems are the key technologies to solve the problem for serving the rapid change in the hard drive industry. Therefore, many rigorous research in the field of robust and high performance control for HDD that can operate under fast data accessing with narrow track pitch is interesting. In addition, imperfection in mechanical components in the hard disk assembly process generates disturbances such as the vibrations of disk media, asymmetric barring and spindle motor, called NRRO (non-repeatable runout) and RRO (repeatable runout). These lead to increase in the amount of PES (position error signal) that limit the performance of the HDD servo system by measuring the variation of the deviation between the center of read/write head and center of the track. Especially the expectation of hard disk prototype with areal density (AD) will be higher than 10 Tb/in^2 before 2020 that was predicted by M. Kryder [1]. That means servo-mechanical system and control method need to support positioning of the R/W head with a PES of a few nanometers while general techniques are not enough. Thus, the modern controls such as robust control are required to attenuate the effect of these

disturbances for increasing servo bandwidth and sustaining the recording density growth. The actuator and HDDs structures are not perfectly rigid that generate disturbance to the HDDs control system. Unpredictable models of disturbance uncertainty give rise to vibrations, which increase the settle time to the target track including position error signal (PES) of HDDs. It has been proved in various itterature that the vibrations exist within a decade of the dynamic model of HDDs interm of resonance frequency, which limit the servo bandwidth and servo performance. Most of these are also the major source of RRO and NRRO disturbance of HDDs. However, there were some researchers investigating to designing the control system in different techniques based on nonlinear control in HDDs actuator, such as mutirate adaptive control of uncertain resonances model by W. Yan et al. in 2016 [5], adaptive feed forward compensation for translation vibration by Y. Luo et al. in 2015 [6], the composite nonlinear feedback (CNF) controller design that index performance by comparing the 3σ PES histograms with the normal PID whose results gain better performance in some senses presented by K. Peng et al. [13] and the optimal fix-order controller for controlling dual state actuator by S.-H. Lee and C. C. Chung in [14]. All of these, proposed the interesting technique to design their controller for sustaining hard drive system in single and dual actuator. Unfortunately, because of time used in head identification technique, complex structure feedback state and uncertainties were not included to design, so it is hard to apply in general industries. Among the various control techniques, linear control based linear matrix equation has been used to analyze system and design plenty of controllers that have been proposed to control a servo system such as the simple structure PI, PID analog control, self-tuning control. Since these techniques do not consider the robustness of the system under various uncertainties, that is, system nonlinear characteristic, resonance frequency including the load changing, the controllers designed that consider robustness and performance of the system are necessary for controlling the HDDs under several uncertainty constraints.

Since over the past two decades, H_∞ control is one of the most well-known techniques in fields of robust control, it is the classical control technique which has high potential to design robust controllers for achieving stability and guaranteed performance of the system. In addition, H_∞ has been widely mentioned and applied in many robust research studies. Although, the robust stability is used to indicate the system stability that achieves in the frequency domain, only this is not enough; so performance, such as steady state error, rise time, and overshoots in term of time should be included to design as well. The integration of these objectives to design the controller has been presented in various techniques for instance H_2/H_∞ optimal procedure [7], μ-synthesis, H_∞ loop shaping, non-smooth, etc. Besides, solving the Riccati equations becomes the essential part of designing the robust controller that was noted in [2,3]. Some successful experiments of H_∞ control applications were presented in [4,7-10]; for example, in [4], D. C. McFarlane and K. Glover proposed a controller designed based loop shaping procedure, and this method used left coprime factorization to model system uncertainties and applied H_∞ to minimizing it. In addition, their system was shaped with the specified loop shaped that depended on designer requirement to achieve better bandwidth and performance including robust stability. However, the structure of their controller is complex and high-order. These studies have shown a number of nominal plant order and compensation order are the main factors of high controller order in H_∞ loop shaping technique. To overcome these problems, lower order of the controller designed have been presented [7-10,15-17], for instance, P. Apkarian et al. [8] presented the application of non-smooth algorithm for designing the fixed-structure centralized PID controller. In [10], H_∞ loop shaping based PSO was applied to MIMO power system with PID structure; in addition, the results of their proposed technique were compared with non-smooth algorithm under centralized and decentralized

constraints, and their results gained more effectiveness of both constraints while the results of the non-smooth usually depend on the initial parameter setting. Additionally, [16] applied their 2dof H_∞ loop shaping controller based GA optimization search with lower order to the head positioning of HDDs, while [17] applied Nanopositioning in small actuator. However, the robust PID structure of their controllers cannot be specified. To overcome these problems above, this paper proposed the novel controller designed that structure order can be specified, which depended on designer requirement. The contributions of this paper include: (1) This paper proposed the designing of robust controller for supporting head positioning in HDDs with the specified order – H_∞ loop shaping synthesis using Particle swarm optimization technique; (2) Proposed controller structure can be specified that is more flexible than the conventional fixed-structure controller; (3) The optimal parameter of proposed controller, $K_{SVCM}(p)$ was automatically searched by using PSO algorithm that utilized stability margin (ε) as the objective function; (4) This technique compared the results under RRO and NRRO disturbance constraint with the similar work such as fixed-structure PID based non-smooth and H_∞ loop shaping based Hankle reduction order technique, and the histogram results demonstrate the proposed specified order technique gains more effectiveness over others.

The paper is arranged as follows. Section 2 details the HDD model with resonance mode and major source of hard disk disturbance, i.e., RROs and NRROs. Section 3 describes the robust controller designed with 4 strategies, classical H_∞ loop shaping synthesis, non-smooth procedure, reduced order by Hankel norm and the proposed specified order – H_∞ loop shaping control. In Section 4, the simulation of the VCM actuator with disturbance testing and the PES in terms of PES histogram is illustrated. Finally, Section 5 summarizes and concludes the results.

2. **Hard Disk Drive System.** Generally, the plant model of HDD can be evaluated that consists of many frequency response to be a lump of the system in the operation [12]. Laser Doppler scanning vibrometer (LDV) is a scientific instrument that is used for measuring the realistic of HDDs plants, whereas a schematic as shown in Figure 1 is a basic principle of laser Doppler scanning vibrometer. At first, the beam of the sensor which has a frequency f_0 is generated from the laser diode source. Beam with frequency f_0 is divided into a reference beam and an inspection beam with beam splitter and then passes through the Bragg cell. Bragg cell is used to add a frequency shift f_b and then the beam 1^{st} fusion of $f_0 + f_b$ is directed to the target. As the motion of the interested target surface (tip of HDDs head) adds a Doppler shift frequency f_d, that is $f_d = 2 \times v\,(t) \times \cos\,(\alpha)\,/\lambda$, where $v(t)$ is the target velocity, α is the angle of laser beam and velocity vector, while λ is the wavelength of the light. This equation illustrates that the changing in frequency and phase of f_d depends on displacement and velocity of test object. Additionally, the scattered light with the 2^{nd} fusion beam of $f_0 + f_b + f_d$ from the tip of head is collected and reflected by the beam splitter to the photo-detector. This scattered light with a 2^{nd} and a reference beam are combined as the superposition that creates the modulate detector output signal revealing the Doppler shift in frequency. Signal processing and analysis of this Doppler are used to measure the tip position of R/W head, including: identify the nominal plan that represents the actual measurement. For each actuator, several frequency response evaluations are plotted experimentally by dynamic signal analyzer (DSA) and used to estimate the frequency response of the realistic measurement as shown in Figure 1. The nominal model of this paper was gathered from the hard disk assembly model from MATLAB, which is a well-known calculated program; the nominal plant is a stable plant with 9^{th} order.

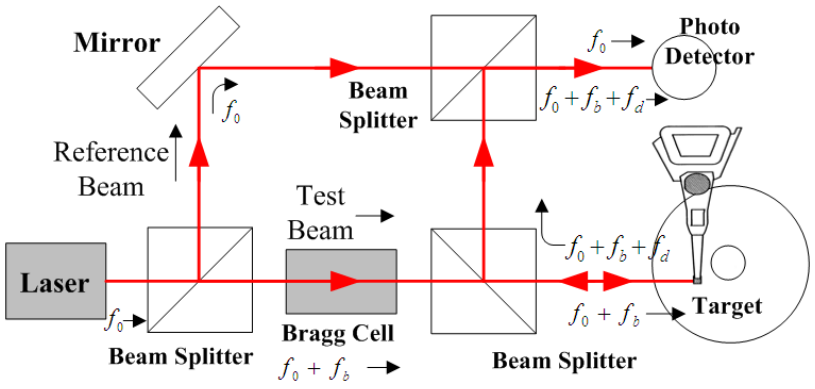

FIGURE 1. Basic diagram of laser doppler scanning vibrometer (LDV) [20]

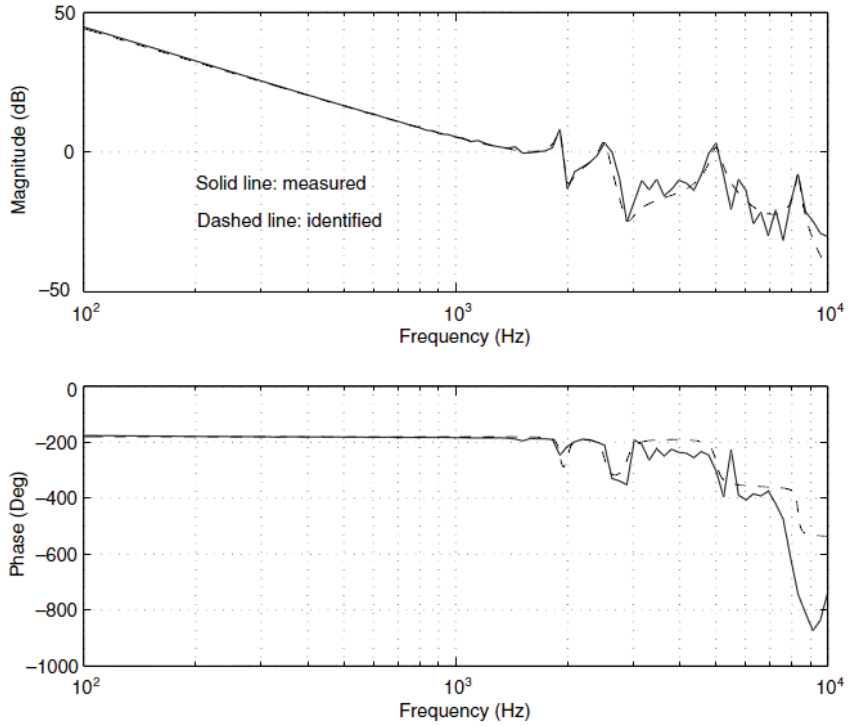

FIGURE 2. The frequency response of the VCM model with resonance modes [11]

The VCM dynamic model can be described as a composite of various high frequency resonance modes that affect the stability of the system. In addition, some of nonlinear characteristics appear in the low frequency caused by pivot-bearing operation. These parameters have to be taken into analysis that is essential for designing the VCM controller. The dynamics model of VCM can be written as follows [11]:

$$\begin{pmatrix} \dot{y} \\ \dot{v} \end{pmatrix} = \begin{bmatrix} 0 & k_y \\ 0 & 0 \end{bmatrix} \begin{pmatrix} y \\ v \end{pmatrix} + \begin{pmatrix} 0 \\ k_y \end{pmatrix} u \tag{1}$$

where y is the position, and v and u are the velocity and input of read/write head, respectively; k_y is position measurement gain while $k_v = k_t/w$, with k_t and w being the current force coefficient and the mass of the VCM actuator, respectively. Therefore, ideal VCM transfer function model is a double integrator stem. However, the resonance modes

are included for the VCM model to achieve the realistic model, and thus:

$$G_v(s) = \frac{K_v K_y}{s^2} \prod_{i=1}^{N} G_{r,i}(s) \tag{2}$$

where N is the number of dominant resonance modes, and $G_{r,i}(s)$ is the i^{th} resonance mode transfer function, that can be formulated as:

$$G_{r,i}(s) = \frac{a_i s^2 + b_i s + \omega_i^2}{s^2 + 2\xi_i \omega_i s + \omega_i^2} \tag{3}$$

where a_i, b_i, ξ_i and ω_i are coefficients of the i^{th} resonance mode dynamic model.

The seeking ID track process is the first process to move the head to the target track; after reaching the wanted tracks, then the controller tries to control the read-write head to stay at the middle of the track; the error of track following affects the PES value [13].

The 3 sigmas of the PES can be converted to the TMR (track miss registration) budget and the TMR budget tends to be smaller since the demand of TPI (track per inch) increased which causes the lower track width. Therefore, the position control system must be designed to be controlled more accurately. The performance of servo drives is based on the results of mechanism of NRRO (non-repeatable runout) and RRO (repeatable runout) which were created by the nature of the track of the servo.

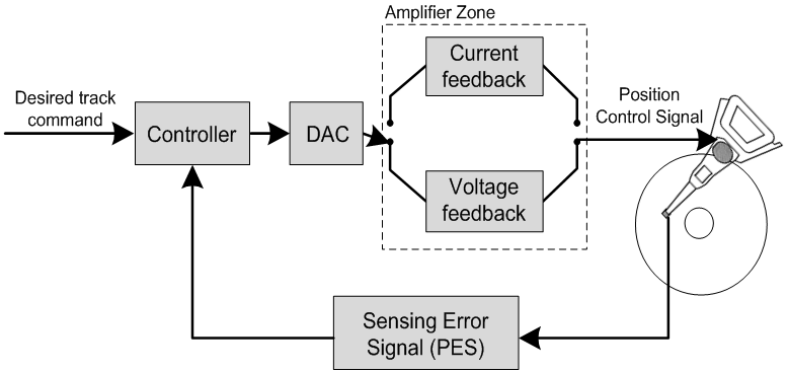

FIGURE 3. The process of the control head positioning read-written on the tracks [13]

Especially, the main factors of NRROs are spindle and bearing defects, wind age included disk flutter and harmonic noise, etc. Some of NRROs affect the resonance frequency changing as shown in Figure 3. In addition, the eccentricity of the track is the major source of RRO, including the motor and bearing geometry that also generate the other RRO sources [11-13]. To be a little more specific, the summation of n sinusoids, $d(t)$ is used to identify the time-varying unknown disturbance of RRO with known frequencies as follows:

$$d(t) = \sum_{i=1}^{n} [a_i(t)\cos(\omega_i t) + b_i(t)\sin(\omega_i t)] \tag{4}$$

3. **H_∞ Loop Shaping Control and Proposed Technique.** The transfer function matrix of co-prime factorization can be used to describe a control feedback behavior, i.e., left co-prime factorization details the control parameter change with state control. Equations (5) and (6) show the state-space of the plant G [2-4]:

$$\dot{x} = Ax + Bu \tag{5}$$

$$y = Cx + Du \tag{6}$$

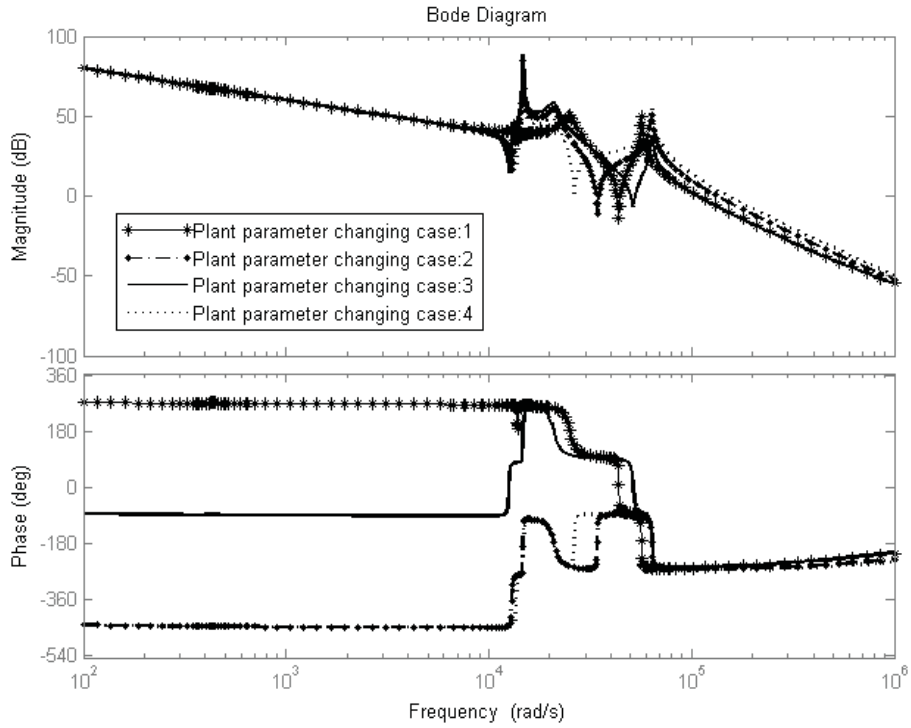

FIGURE 4. The frequency response of the RRO & NNRO affecting the resonance modes

Left coprime factor is considered for controlling the nominal plant of the HDD system as follows:

$$\begin{bmatrix} \tilde{N} & \tilde{M} \end{bmatrix} = \left[\begin{array}{cc|c} A+LC & B+LD & L \\ ZC & ZD & Z \end{array}\right] \tag{7}$$

where Z can be any nonsingular matrix. In addition, $Z = (I + DD^*)^{-1/2}$ can be chosen if $G_{VCM} = \tilde{M}^{-1}\tilde{N}$ is defined to be a normalized left-coprime factorization and then a perturbed model can be written as:

$$G_{VCM}(s) = \left(\tilde{M} + \Delta_M\right)^{-1} \left(\tilde{N} + \Delta_N\right) \tag{8}$$

where G_{VCM} is a normalized left coprime factorization of the nominal VCM plant, and Δ_M, Δ_N are uncertainty transfer functions of system, with which it can investigate a group of structure with the following description:

$$\xi_\varepsilon = \left\{ G_{VCM} = \left(\tilde{M} + \Delta_M\right)^{-1} \left(\tilde{N} + \Delta_N\right) : \|\Delta_M \Delta_N\|_\infty < \varepsilon \right\} \tag{9}$$

where $\gamma_{\min}$ is the maximum stability margin. The greatest value of $\gamma = \gamma_{\min}$ or $\varepsilon_{\max}$ is the target of finding an optimal solution for example all the models belonging to ξ_ε can be stabilized by controller K_∞. The synthesis of optimal controller K_∞ and $\gamma_{\min}$ that stabilized $G_{VCM}(s)$ are as:

$$\left\| \begin{pmatrix} I \\ K \end{pmatrix} (I - G_{SVCM}K)^{-1} (IW_2 G_{VCM} W_1) \right\|_\infty = \gamma_{\min} = \varepsilon_{\max}^{-1} \tag{10}$$

That is equivalent to

$$\left\| \begin{bmatrix} KS_s & KS_sS_s \\ S_s & S_sG_{SVCM} \end{bmatrix} \right\|_\infty \leq \varepsilon_{\max}^{-1} \tag{11}$$

where $S_S = (I - G_{SVCM}K)^{-1}$. The objective of this 4-block fitness function is to incorporate the simple performance/robustness tradeoff that guarantees the stability of H_{inf} procedure, developed by McFarlane and Glover. Nevertheless, they also suggested the minimal value $\gamma_{\min}$ should be less than 4 in the MIMO system and the calculation is given by:

$$\gamma_{\min} = \frac{1}{\sqrt{1 - \lambda_{\max}(YQ)}} = \left(1 - \left\| \left[\tilde{N}\ \tilde{M}\right] \right\|_H^2\right)^{-1/2} \tag{12}$$

where $\lambda_{\max}$ represents the greatest eigenvalue of YQ. Moreover, for any values $\gamma > \gamma_{\min}$, a corrector stabilizing all the models belonging to ξ_ε is given by:

$$K_\infty(s) = B^T X \left(sI - A + BB^T X - \gamma^2 ZYC^T C\right)^{-1} \gamma ZYC^T \tag{13}$$

$$Z = (I + YX - \gamma^2 I)^{-1} \tag{14}$$

where Y, Q are the solutions of the Riccati equations while A, B and C represent the state matrices of the shaped plant defined by the function G_{VCM}.

3.1. **The loop shaping design procedure.** The calculation of the normalized co-prime factorization and the synthesizing of H_∞ robust loop shaping design can be seen in [5]. The performance in terms of loop shaping must be specified before calculating the pre/post weighting functions. The design procedure can be briefly described as follows.

• The nominal plant $G_{VCM}(s)$ is used to be controlled by selecting the pre/post weighting function for shaping the desired open loop plant. The shaping plant with pre/post weighing function are combined in order to improve the performances of the system such as $G_{SVCM}(s) = W_2(s)G_{VCM}(s)W_1(s)$.

• Synthesize the controller, K_∞ ensuring the stability margin γ slightly more than $\gamma_{\min}$.

• Combine the H_∞ controller, K_∞, with the shaping functions as the final feedback controller such that:

$$K_{SVCM}(s) = W_1(s)K_\infty(s)W_2(s) \tag{15}$$

3.2. **Non-smooth technique for H_∞ design algorithm.** In this section, the non-smooth optimization was presented for solving H_∞ designed problems with structural controller constraint. The major advantages of this technique are the avoidance for using Lyapunov variables and the size reduction of optimization programs even for very large systems. This algorithm applies bundling approaches and generalized gradients that are suitable for the computed descent directions and norm by solving the problems of quadratic programs and creating a step off line search. See [7-9] for a more detailed discussion; briefly, they start with the composite functions $f = \|\cdot\|_\infty \circ T_{w\to z}$ or more generally $g = \|\cdot\|_\infty \circ T_{w\to z} \circ \chi(\cdot)$ are written as a form:

$$g(\kappa) = \max_{\omega\in[0,+\infty]} g(\kappa, \omega) \tag{16}$$

where $g(\kappa, \omega)$ is a function of maximum singular value composition. The steps of this method to minimize $g(\kappa)$ were illustrated in [8]. Moreover, the non-smooth technique was applied to synthesizing the fixed structure PID robust controller for hard disk drive 9^{th} order model. From [9] the feedback loop was used to position the head on the correct track of HDD. This control structure consists of a PID controller and a low-pass filter in the return path as shown in Figure 5.

Based on classical H_∞ loop shaping design and non-smooth algorithm, the controller PID and filter were tuned to achieve the performance of loop shaping LS and the robustness of H_∞ synthesis. In this paper, the results of this strategy were investigated in terms of performance.

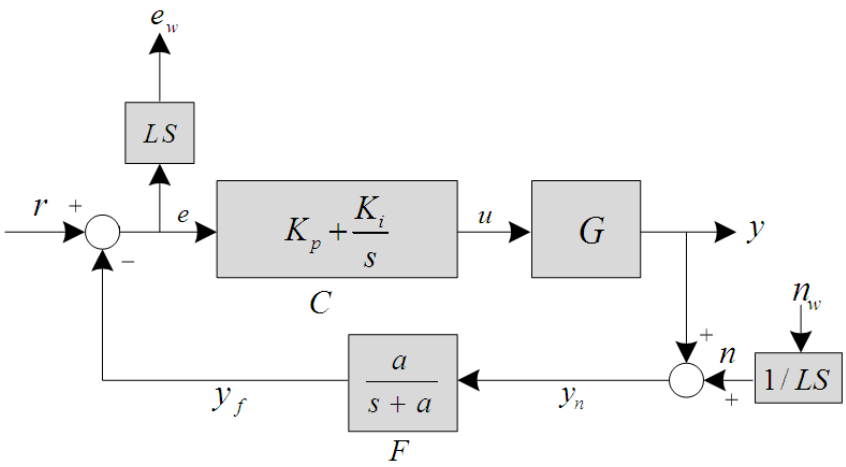

FIGURE 5. Closed-loop formulation of non-smooth for hard disk drive assembly [7]

3.3. **Specified order – H_∞ loop-shaping based particle swarm optimization (SO-HLS).** In this research, a specified order – H_∞ robust loop shaping control (SOHLS) is applied to the VCM servo system under RRO and NRRO disturbances. The conventional strategy can be applied to generating the desired loop shaping controller; however, they are still complicated with high order. The set of parameters, p, in the controller $K_{SVCM}(p)$ is attempted to be evaluated while pre/post weighting function W_1 and W_2 are selected manually based on the classical loop shaping technique [4]. For inverting Equation (15), thus K_∞ can be rewritten as:

$$K_\infty(s) = W_1^{-1}(s)\, K_{SVCM}(s)\, W_2^{-1}(s) \tag{17}$$

Substitute (17) into (10), and the infinity-norm of disturbances to states transfer function can be written as:

$$\left\| \begin{bmatrix} I \\ W_1^{-1} K_{SVCM}(p) W_2^{-1} \end{bmatrix} \left(I - G_{SVCM} W_1^{-1} K_{SVCM}(d) W_2^{-1}\right)^{-1} M_s^{-1} \right\|_\infty^{-1} \tag{18}$$

PSO [18] is the effective method to analyze the nonlinear optimization problems. This method adapts the concept of particles y around the problem space until getting the stopping condition. The improved fitness function of this method is used to identify the best solution (particle). In the proposed technique, the parameters set p is formulated like a particle, and the fitness condition can be written as:

$$f_s = \left\{ \begin{array}{ll} \varepsilon & \text{for } K(d) \text{ stabilizing the plant.} \\ 1 \times 10^{-5} & \text{Othercase.} \end{array} \right\} \tag{19}$$

The fitness function is biased to be a small value if there is at least one constraint not met. Based on the specifications above, this proposed method can be described as follows.
• Identify the parameters of particle swarm optimization, i.e., population size in particle swarm, min-max values of the bounded space: ($x_{\min}$, $x_{\max}$, $p_{\min}$, $p_{\max}$), min-max weights inertia ($Q_{\min}$, $Q_{\max}$), min-max particle velocity ($v_{\min}, v_{\max}$), and set max iteration ($i_{\max}$) and acceleration coefficients (α_1, α_2).
• Initialize 1^{st} particles, randomly.
• Estimate the fitness function ($f's$) for each particle; and the best value found by particle i, call it as Pb, and search the greatest value with the swarm, called Ub.

• Update the inertia weight (Q) as:

$$Q = Q_{\max} - \left(\frac{Q_{\max} - Q_{\min}}{i_{\max}}\right) i \tag{20}$$

Update the position (p) and velocity (v) of each particle.

$$v_{i+1} = Q_{vi} + \alpha_1 \left[\gamma_{1i}(P_b - p_i)\right] + \alpha_2 \tag{21}$$

$$p_{i+1} = p_i + v_{i+1} \tag{22}$$

where α_1, α_2 are the specified acceleration coefficients and γ_{1i}, γ_{2i} are the numbers from the random search.

• Increase the working iteration for a step ($i = i + 1$). If the current iteration is the maximum iteration $i = i_{\max}$, then stop. If not, start to evaluate the fitness function $f(s)$ again.

4. **Simulation Results of HDD Servo System.** In this section, the proposed SOHLS technique is applied to controlling the hard disk servo system. To illustrate the performance and robustness of the system, the comparison of three controllers designed are shown in type of step response and concluded in the figure of histograms. The dynamic model of the VCM actuator of this paper can be written as:

$$Gp = \left\{ \frac{\begin{array}{c} 1.544 \times 10^{09} s^7 + 1.051 \times 10^{15} s^6 + 3.087 \times 10^{18} s^5 + 2.202 \times 10^{24} s^4 \\ + 9.03 \times 10^{26} s^3 + 3.886 \times 10^{32} s^2 + 1.723 \times 10^{34} + 7.466 \times 10^{37} \end{array}}{\begin{array}{c} s^9 + 3273 s^8 + 4.023 \times 10^{09} s^7 + 9.74 \times 10^{12} s^6 + 2.754 \times 10^{18} s^5 \\ + 2.04 \times 10^{21} s^4 + 3.866 \times 10^{26} s^3 + 2.217 \times 10^{28} s^2 \\ + 7.488 \times 10^{31} s + 9.332 \times 10^{32} \end{array}} \right\} \tag{23}$$

Pre-compensator, W_1 is selected for attenuating the disturbance at lower crossover frequency with high gain as a post-compensator, W_2 is used for reducing the effect of measurement noise with low gain at high frequency. Considering the loop shape of the plant in (23), the pre/post weight function W_1 and W_2 were chosen as:

$$W_1 = \frac{0.00809s + 56.95}{s + 5900} \tag{24}$$

$$W_2 = \frac{s + 39300}{s + 217500} \tag{25}$$

The controller designed by the conventional robust loop shaping technique provides a 12^{th} order controller and the best infinity norm and stability margin of this loop shaping method are $\gamma_{\min} = 1.7653$ and $\varepsilon_{\max} = 0.704$, respectively. Clearly, the selected weight is compatible with the robust stabilization control problem; however, the 12^{th} order of conventional controller is quite complicated for implementation.

The classic controller based on H_∞ loop shaping, K_{SVCM} that robustly stabilizes the shaped plant G_{SVCM} is synthesized as:

$$K_{SVCM}(s) = \left\{ \frac{\begin{array}{c} 0.008138 \times s^{12} + 2216 \times s^{11} + 1.351 \times 10^8 s^{10} + 1.01 \times 10^{13} s^9 \\ + 4.334 \times 10^{17} s^8 + 1.072 \times 10^{22} s^7 + 2.905 \times 10^{26} s^6 \\ + 3.71 \times 10^{30} s^5 + 4.66234 \times s^4 + 3.846 \times 10^{38} s^3 \\ + 1.135 \times 10^{42} s^2 + 1.211 \times 10^{44} s + 2.136 \times 10^{47} \end{array}}{\begin{array}{c} s^{12} + 4.552 \times 10^5 s^{11} + 6.025 \times 10^{10} s^{10} + 2.826 \times 10^{15} s^9 \\ + 2.29 \times 10^{20} s^8 + 4.82 \times 10^{24} s^7 + 1.642 \times 10^{29} s^6 \\ + 2.033 \times 10^{33} s^5 + 2.702 \times 10^{37} s^4 + 2.293 \times 10^{41} s^3 \\ + 6.649 \times 10^{44} s^2 + 7.232 \times 10^{46} s + 1.249 \times 10^{50} \end{array}} \right\} \tag{26}$$

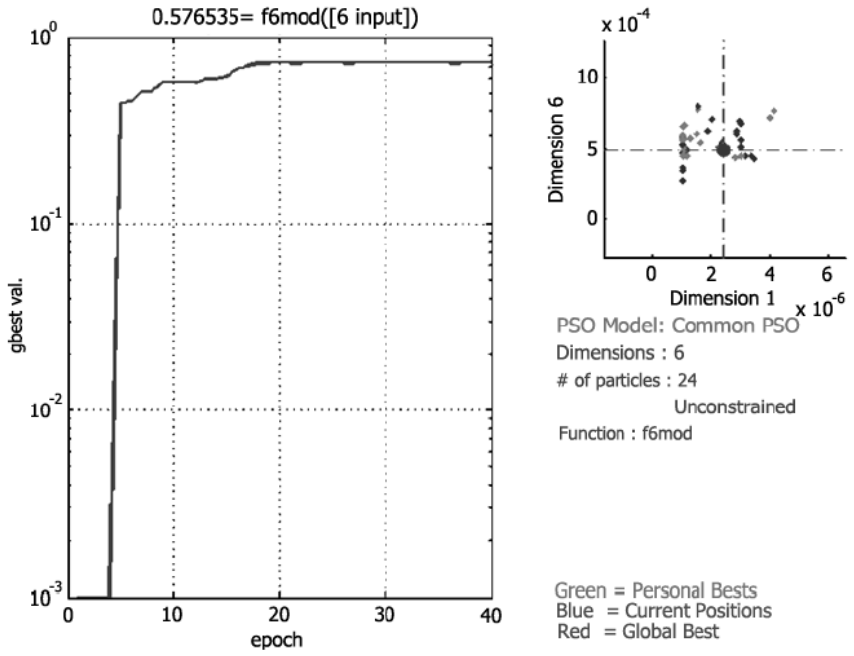

FIGURE 6. Fitness functions gbest versus iteration in the PSO

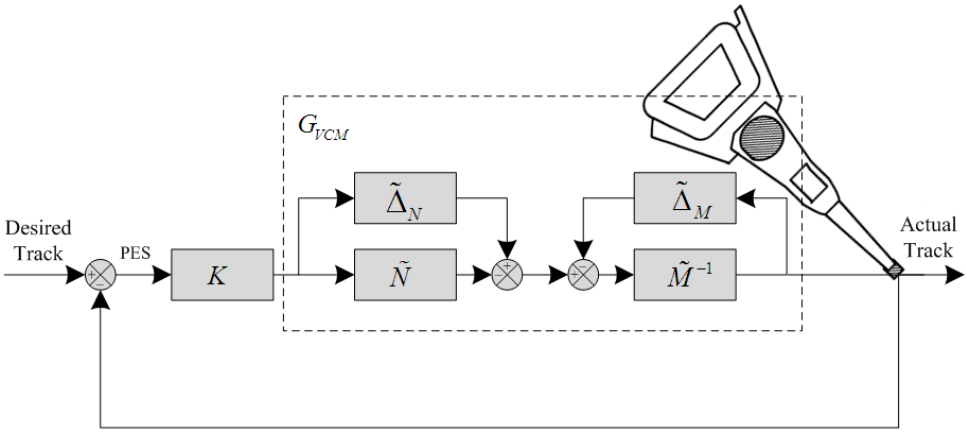

FIGURE 7. Coprime factor robust stabilization problem

Due to the fact that the 12th order of the classic controller above affects time calculation of the system that causes increase in the data access time of HDD, the widely used technique, Hankel norm model reduction strategy, was applied for decreasing the order of K_{SVCM} from the 12th order to 3rd, and the reduced order controller can be written as:

$$K_{REDUCE} = \left\{ \frac{0.008138s^3 + 219.9s^2 + 2.571 \times 10^7 s + 6.946 \times 10^{11}}{s^3 + 2.865 \times 10^5 s^2 + 3.259 \times 10^9 s + 8.984 \times 10^{14}} \right\} \tag{27}$$

The position of measured PES, actual position and the controller are shown in Figure 7. Although, the reduction controller is the third-order controller, that solves the problem of complicated and high order controller structure; however, the stability margin and performance are quite degraded. The stability margin is reduced to 0.4118. In addition, the controller of non-smooth technique with PI structure and first order filter that were described in Section 3.2 were designed and the resulting controllers are:

$$K_{NONSMOOTH} = \left\{ 0.000846 + \frac{0.0103}{s} \right\} \tag{28}$$

$$F_{NONSMOOTH} = \left\{ \frac{5486}{s + 5486} \right\} \tag{29}$$

Finally, the proposed SOHLS controller evaluated from the PSO was carried out and the structure of the controller was demonstrated in (30), in which K_1-K_8 are the parameters to be evaluated.

$$K_{SOHLS}(p) = \left\{ \frac{K_1 s^3 + K_2 s^2 + K_3 s + K_4}{K_5 s^3 + K_6 s^2 + K_7 s + K_8} \right\} \tag{30}$$

In the optimization problem, PSO parameters were speicified as follows: the upper and lower bounds of the PSO and parameters are set as follows: $K_1 \in [0.001, 0.01]$, $K_2 \in [10, 1000]$, $K_3 \in [100, 10000]$, $K_4 \in [100, 100000]$, $K_5 \in [1, 100]$, $K_6 \in [1000, 200000]$, $K_7 \in [1000, 200000]$, $K_8 \in [1000, 200000]$, population size = 24, min-max velocity are 1 and 3, respectively, acceleration value = 2.1, minimum and maximum inertia are 0.3 and 0.7, respectively, iteration limit as 50. The obtained optimal solution is shown in (18), which has the stability margin $\varepsilon_{otp} = 0.5765$. Clearly, the stability margin of the proposed controller is nearly to the full order controller (12^{th} controller). The optimal controller of the proposed SOHLS can be written as:

$$K_{SOHLS}(p) = \left\{ \frac{0.001275s^3 + 275.4s^2 + 2580s + 5.037 \times 10^4}{15s^3 + 140000s^2 + 2.291 \times 10^5 s + 1.198 \times 10^5} \right\} \tag{31}$$

Figure 6 shows convergence of fitness function curves that indicates the solution is the converged and the stability margin is the optimal value. The optimal SOHLS controller provides a satisfied stability margin that is greater than the reduced order with the similar controller structure as seen in Table 1.

TABLE 1. The performance and robustness specifications of the controller designed

Type of controller	***Settling time***	***Over shoot***	***Stability margin***
Full order HLS	*0.0023*	*0.0848*	*0.704*
Reduced order	*0.0052*	*0.0725*	*0.4118*
Proposed SOHLS	*0.0017*	*0*	*0.5765*
Non-smooth	*0.0039*	*0*	*0.6410*

The open loop Bode diagrams are used to verify the performance in the frequency domain of all controllers. The comparison of the nominal plant G_{VCM} with the shaped desired plant G_{SVCM} is shown in Figure 8(a). The H_∞ loop shaping and the loops shaped by three different techniques are plotted in Figure 8(b). Clearly, the proposed SOHLS performs as robust controller, in which its loop shaping is quite similar to the shape of the conventional robust loop controller. Figure 8(c) shows the step responses of the optimal solution from the robust non-smooth, the proposed robust SOHLS, the reduced 3^{rd} order and conventional H_∞ loop shaping controller. As seen in this figure, the proposed SOHLS provides a better performance than that of other tested techniques. The details of this step response are described in Table 1.

The disturbances in the actual HDD are usually interesting as a group of plant output disturbance, called runouts. Repeatable runouts (RROs) and non-repeatable runouts (NRROs) are the main factors of track following errors. Generally, the pattern of NRROs is hardly predictable that depends on the nature, unlike repeatable runouts. A perfect HDD servo system should use the controller that can attenuate both of NRROs and RROs disturbances.

In case of the robustness testing to attenuate the RRO and NRROs disturbances, the runouts were considered to be added to the simulation. Based on several literature

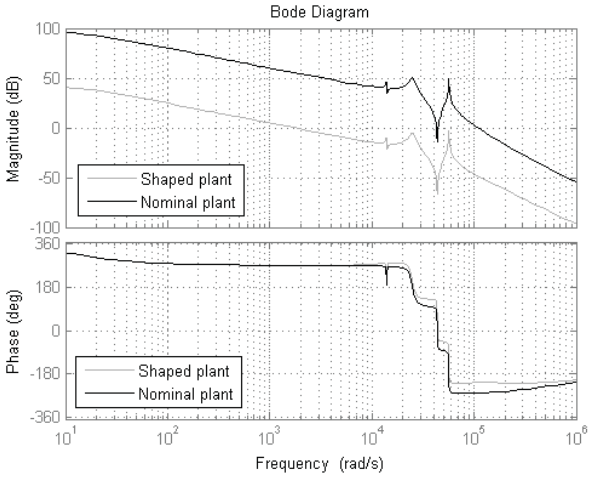

(a) Desired loop shaping and nominal plant

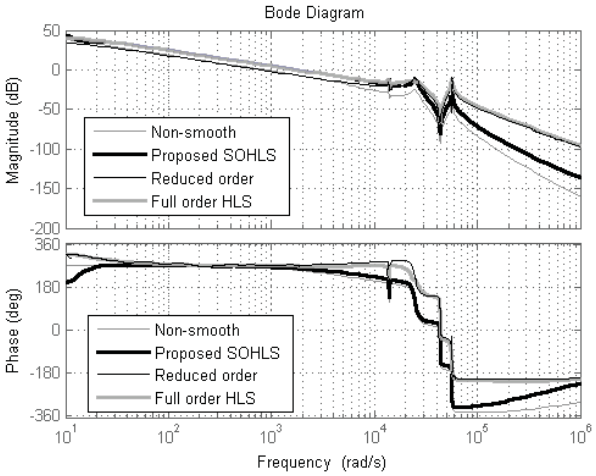

(b) Comparison of robust non-smooth, proposed robust SOHLS, reduced 3rd order and conventional H_∞ loop shaping controller

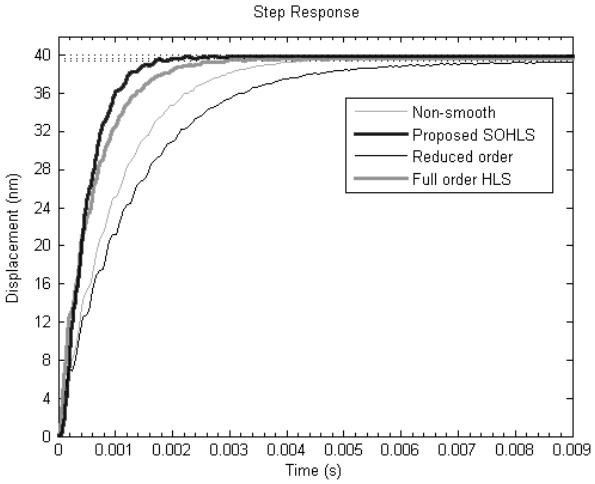

(c) Step responses of robust non-smooth, proposed robust SOHLS, reduced 3rd order and conventional H_∞ loop shaping controller

FIGURE 8. Bode of (a) nominal plant and shaped plant, (b) open loop plot of controllers, and (c) step responses of controllers

studied, the runouts in actual hard disk drives are the majority consisting of RROs as the basic summation of sinusoidal with fundamental frequency 55 Hz, equivalent to the spindle motor speed [13]. The signal of PES with fictitious runouts can be written as:

$$d(t) = 0.5 + 0.1\cos(110\pi t) + 0.05\sin(220\pi t) + 0.02\sin(440\pi t) + 0.01\sin(880\pi t) \quad (32)$$

This signal was added to the output with the zero mean reference signal. The position signal to be considered is the position error signal (PES). The statistic methodology such as 3σ PES (standard deviation) is a suitable parameter used to analyze the deviation of head position. Figures 9 and 10 show the output responses and the position error signal (PES) histograms, respectively. As seen in Figure 9, the proposed controller can attenuate the disturbances from both RRO and NRROS within 2.5 nms while the reduced order controller and the controller designed by non-smooth technique fail to stabilize the system under the presence of disturbances. Figure 10 shows the statistical distribution of the PES under RROs for all controllers. For the distribution under NRROs and RROs,

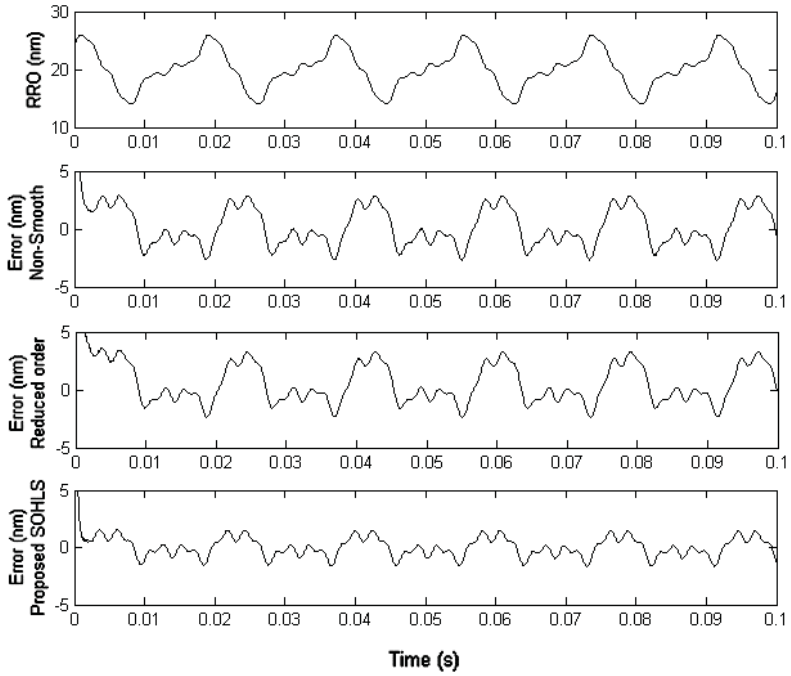

(a) Comparison PES of the proposed SOHLS, non-smooth and reduced order controllers under the only RROs constraint

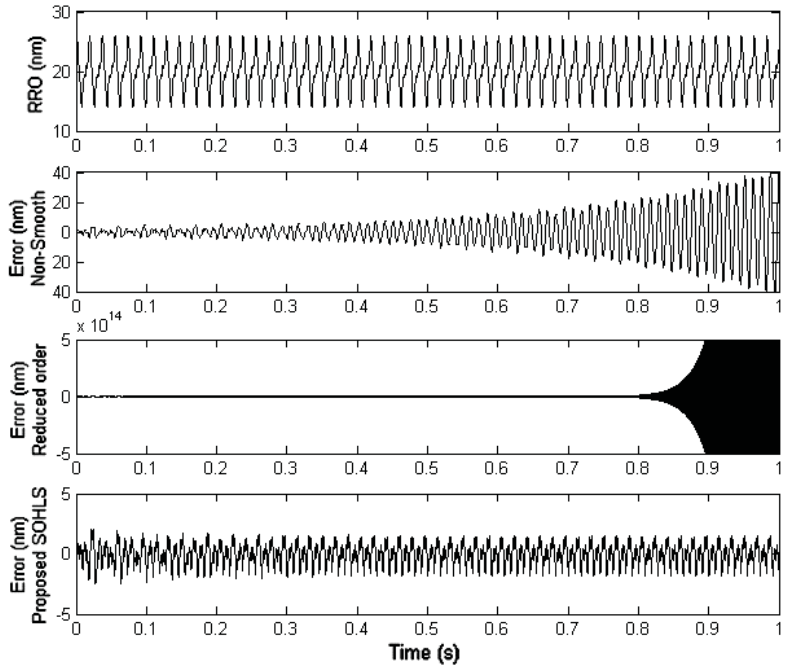

(b) Comparison PES of the proposed SOHLS, non-smooth and reduced order controllers under both RROs and NRROs with resonance shifting constraint

FIGURE 9. Output response under runouts disturbances: (a) comparison PES under the only RROs constraint, (b) comparison PES under the RROs and NRROs constraints

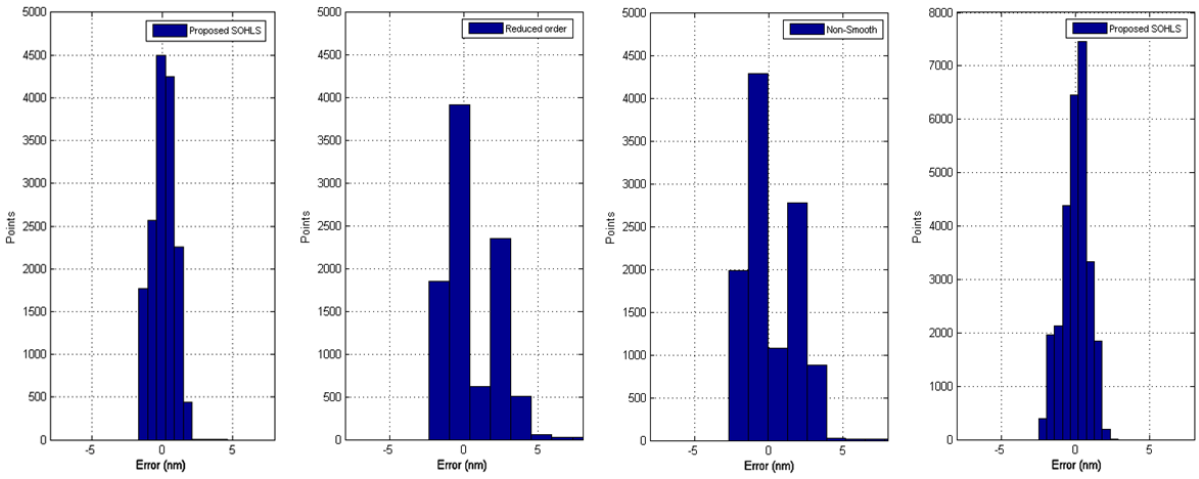

(a) (b) (c) (d)

FIGURE 10. Comparison of σ_{PES} histograms of three algorithms: (a) the proposed SOHLS with RROs, (b) reduce order by Hankel norm with RROs, (c) non-smooth technique with RROs and (d) the proposed SOHLS with RROs and NRROs disturbances.

TABLE 2. The $3\sigma_{PES}$ of the PES testing

Type of controller	***$3\sigma_{PES}$ (nm) of RROs test***	***$3\sigma_{PES}$ (nm) of RROs and NRROs test***
Proposed SOHLS	*2.5110*	*2.5423*
Reduced order 3^{rd} order	*5.0168*	*N/A*
Non-smooth	*4.8575*	*N/A*

only the result from the proposed SOHLS can be presented since the outputs from the reduced order and a non-smooth controllers are unstable under this condition. Table 2 also illustrates the $3\sigma_{PES}$ value of several interested techniques after testing, which were obtained by measuring the PES. Moreover, $3\sigma_{PES}$ is the main factor to indicate the maximum achievable track density and also shows the performance of the controller designed.

5. **Conclusions.** This paper proposes the specified order – H_∞ loop shaping (SOHLS) applied to the HDD servo system that can achieve a better performance system for attenuating the effect of RROs and NRROs disturbance. As illustrated in the results, it is clearly shown that the SOHLS controller designed achieves good robust performance. Although the design of the robust SOHLS controller is not easy to be carried out by mathematical methods, due to the nature of nonlinear problem, the particle swarm optimization simplifies this difficulty by finding the best solution based on swarm searching technique. The value of ε after running the PSO of SOHLS is 0.5765, indicating that the designed controller is suitable for the specified open loop shaping method and also guarantees the robustness. Although the ε of the conventional H_∞ robust loop shaping is 0.704 which is more than that of the proposed technique; however, the conventional controller is complicated with the 12^{th} order controller and it is difficult for implementation. Moreover, the statistical data $3\sigma_{PES}$ value of the PES indicates the successful controller, which can attenuate both the RROs and NRROs. The results demonstrate that the robust performance of the proposed SOHLS is better than that of the reduced order controller by Hankel norm and non-smooth method against the counterpart condition.

Acknowledgments. This work is supported by the Thailand Research Fund under the research grant No. PHD57I0052 and Seagate Technology (Thailand) Co. Ltd. Moreover, Department of Electrical Engineering of KMIT'L, Bangkok, Thailand.

REFERENCES

[1] M. Kryder, *Seventy Years of Disk Drives: The Exciting Road Ahead, Seagate Technology*, 2006.
[2] S. Skogestad and I. Postlethwaite, *Multivariable Feedback Control Analysis and Design*, 2nd Edition, John Wiley & Sons, New York, 1996.
[3] K. Zhou and J. C. Doyle, *Essential of Robust Control*, Prentice-Hall, 1998.
[4] D. C. McFarlane and K. Glover, A loop shaping design procedure using H_∞ synthesis, *IEEE Trans. Automatic Control*, vol.37, no.6, pp.759-769, 1992.
[5] W. Yan, C. Du and C. K. Pang, Multirate adaptive control of uncertain resonances beyond the Nyquist frequency in high-performance mechatronic systems, *Automatica*, vol.66, pp.63-72, 2016.
[6] Y. Luo, T. Zhang and L. Zhou, Pre-filtering and head-dependent adaptive feed-forward compensation for translation vibration in hard-disc-drive, *Mechatronics*, vol.27, pp.13-19, 2015.
[7] S. J. Ho, M. H. Hung, L. S. Shu and H. L. Huang, Designing structure-specified mixed H_2/H_∞ optimal controllers using an intelligent genetic algorithm, *IEEE Trans. Control Systems*, vol.13, pp.1119-1124, 2005.
[8] P. Apkarian and V. Bompart, Nonsmooth structured control design with applications to PID loop shaping of a process, *International Journal of Robust and Nonlinear Control*, vol.17, pp.1320-1342, 2007.
[9] N. A. Bruisma and M. Steinbuch, A fast algorithm to compute the H_∞ – Norm of a transfer function matrix, *System Control Letters*, vol.14, pp.287-293, 1990.
[10] S. Kaitwanidvilai, Particel swarm optimization based fixed-structure H_∞ loop shaping control of MIMO system, *Proc. of IASTED Internatioanal Conference*, Innsbruck, Austria, pp.207-212, 2008.
[11] M. Ben, T. H. Lee, V. Venkatakrishnan and P. Kemao, *Hard Disk Drive Servo Systems*, 2nd Edition, Springer, 2005.
[12] W. Guo, S. Weerasooriya, T. B. Goh, Q. H. Li, C. Bi and K. T. Chang, Dual stage actuators for high density rotating memory devices, *IEEE Trans. Magn.*, vol.34, pp.450-455, 1998.
[13] K. Peng, B. M. Chen, V. Venkataramanan and T. H. Lee, Design and implementation of a dual-stage actuated HDD servo system via composite nonlinear control approach, *Mechatronics*, vol.14, pp.965-988, 2004.
[14] S.-H. Lee and C. C. Chung, Optimal design and testing of a digital dual-stage actuator servo system, *IET Control Theory and Applications*, vol.4, pp.2029-2040, 2010.
[15] H. Li, C. Du and Y. Wang, Optimal reset control for a dual-stage actuator system in HDDs, *IEEE Trans. Mechatronics*, vol.16, no.10, pp.480-488, 2011.
[16] S. Kaitwanidvilai and A. Nath, Design and implementation of a high performance hard disk drive servo controller using GA based 2DOF robust controller, *International Journal of Innovative Computing, Information and Control*, vol.8, no.2, pp.1025-1036, 2012.
[17] S. S. Aphale, S. O. R. Moheimani and A. Ferreira, A robust loop-shaping approach to fast and accurate nanopositioning, *Sensors and Actuators A: Physical*, vol.204, pp.88-96, 2013.
[18] J. Kennedy and R. Eberhart, Particle swarm optimization, *Proc. of IEEE International Conference on Neural Networks*, Perth, Australia, vol.4, pp.1942-1948, 1995.
[19] Y. Hamada and K. Date, Disk storage device, *US Patent No. 6989957*, 2009.
[20] R. Li, T. Wang, Z. Zhu and W. Xiao, Vibration characteristics of various surfaces using an LDV for long-range voice acquisition, *IEEE Sensors Journal*, vol.11, no.6, pp.1415-1422, 2011.